JMEPEG (2009) 18:1052–1059
DOI: 10.1007/s11665-009-9352-7

1059-9495/$19.00

Nature of Surface Changes in Stamping Tools of Gray and Ductile Cast Iron During Gas and Plasma Nitrocarburizing

E. Roliński, A. Konieczny, and G. Sharp

(Submitted October 28, 2008; in revised form December 17, 2008)

Two cast irons, pearlitic-ferritic gray and ferritic ductile, were plasma and gas nitrocarburized at the same temperature and for the same processing time to produce a compound zone of about 10-14 μm thick. It was demonstrated that both processes caused changes in the surface roughness of the irons, and the most dramatic increase of roughness was observed after gas nitrocarburizing of the gray cast iron. It was shown that the primary reason that the results were not the same is the difference in the nitriding mechanism. Significant penetration of the surface voids and imperfections between the graphite particles and the metallic matrix by ammonia molecules led to the formation of a locally thicker compound zone and a bulging of the metallic matrix above the surface. This phenomenon did not occur in the plasma process and as a result the surface changes were much smaller than in the gas process.

Keywords cast irons, gas nitrocarburizing, heat treating, plasma nitrocarburizing, surface engineering, surface roughness

1. Introduction

Surface hardening of cast irons by nitriding/nitrocarburizing methods has recently attracted renewed attention since those materials are often used to make large dies for metal-forming applications (Ref 1). Due to continuously challenging demand for stamped auto-body parts made of much stronger steels such as TRIP, Dual Phase, and others, the automotive industry is in need for more durable tools (Ref 1). Cast irons are occasionally nitrided for many other applications with the aim of enhancing surface hardness and corrosion resistance of the products (Ref 2). Therefore, a better understanding of the existing processes, applied to cast iron materials, may lead to their optimization for tooling in the metal-forming industry.

The mechanism of adsorption of the active nitrogen species on the surface of structurally discontinuous materials such as various cast irons has an important effect on their surface structure and properties (Ref 1). Thus such materials might also be good models for exploration of the phenomenon. Although the mechanism of plasma nitriding has been the subject of intense studies for a number of years, its actual understanding is still controversial (Ref 3-13). It is not absolutely clear if the mechanism of plasma nitriding relies solely on the formation of the active nitrogen species from the N_2^+ ions, dominating ionic spectrum of the near-cathode region of the glow discharge (Ref 3), or on reactive sputtering (Ref 5). It is, however, clear that the creation of those species depends on the formation of the unrestricted cathode fall region in proximity to the nitrided surface, which requires sufficient space to occur (Ref 14). The thickness of the cathode fall region depends mainly on the pressure of the processing gas and it is in the order of millimeters. As a result the glow discharge cannot exist in stable form in any of the cracks, gaps, and the other millimeter-size or smaller surface defects existing on the material, since their dimensions are smaller than the thickness of the cathodic fall.

At the same time, plasma also generates active nitrogen atoms near the surface as a result of direct contact of ions impinging on the solid or from the deposited Fe-N iron nitride clusters formed above the cathode, arising from the reactive sputtering (Ref 5).

The mean free-path or mean free-lifetime of all these active species, ions, and atoms is insufficient to allow penetration of those surface defects. These species undergo neutralization at the surface and therefore the plasma method is not very effective in penetrating various surface cracks or bulk porosities. Ammonia molecules, on the contrary, may penetrate such defects before cracking and cause internal nitriding.

It can be expected that surface penetration in these methods may look like the mechanism shown in Fig. 1. Gas nitriding has long been established as a process, which begins by chemisorption on the iron surface of ammonia molecules, followed by their gradual dehydrogenation and then a diffusive absorption of active nitrogen atoms (Ref 15). If the formations of active nitrogen species such as nitrogen atoms were possible in the above-mentioned cavities during plasma nitriding, there would not be any differences in results between plasma and gas nitriding processes.

However, there are a number of empirical observations proving that those differences do exist. A good example of that

E. Roliński, Advanced Heat Treat Corp., 1625 Rose Street, Monroe, MI 48162; **A. Konieczny**, U S Steel Automotive Center, 5850 New King Court, Troy, MI 48098; and **G. Sharp**, Advanced Heat Treat Corp., Waterloo, IA. Contact e-mails: doctorglow@ion-nitriding.com, AKonieczny@uss.com, sharpg@ion-nitriding.com.

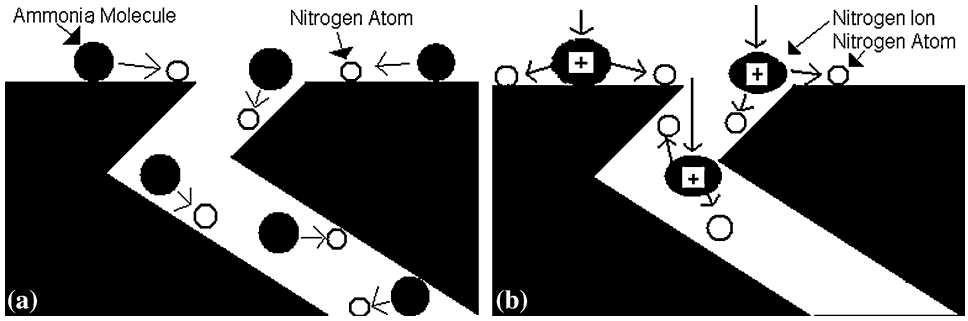

Fig. 1 Hypothetical penetration of the surface cavity and formation of the active nitrogen atoms: (a) in gas nitriding from ammonia molecules; (b) in plasma nitriding from N_2^+ ions

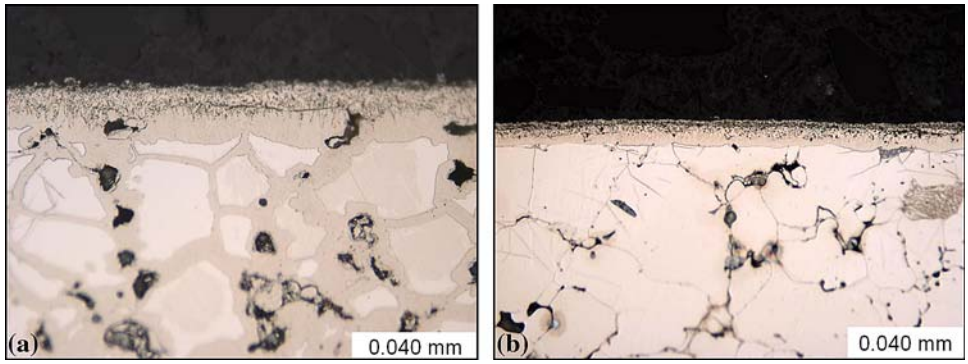

Fig. 2 Optical photomicrographs of the Fe-0.8%P sintered material after nitrocarburizing at 566 °C (1050 °F) in gas (a) and in plasma (b). Note the porous nature of the alloy and the nitrided layer deeply penetrating into the gas treated sample. Etched with 3% nital

is a comparison of the powder metallurgy (PM) metal treated by both the plasma and gas methods as shown in Fig. 1(a) and (b). The Fe-0.8%P sintered material sample with a density of 7.2 g/cm^3 has been thoroughly penetrated and internally nitrided by ammonia (Fig. 2a) while plasma nitrocarburizing was limited only to the surface (Fig. 2b). This fact also underscores that the application of plasma methods to variety of PM sintered components requiring surface treatment is fully justified (Ref 16, 17).

Gray cast and ductile irons contain graphite in different forms, which may become detached from the matrix during machining. The resulting interface between these structural components may not be as tight near the surface as at the core (Ref 18, 19). Open porosity, cracks, and similar defects are prone to penetration by ammonia (Ref 1, 20). If so, nitriding/nitrocarburizing with ammonia may lead to significant surface structure and geometry changes. The investigation of these changes in the gray and ductile cast irons during gas and plasma nitriding was the subject of our studies.

2. Experiments

2.1 Samples Preparation

The materials investigated were cast materials used for stamping dies: alloyed pearlitic-ferritic gray cast iron G3500/NAAMS and non-alloyed ferritic ductile iron D4512/NAAMS (Ref 21) with the chemical composition shown in Table 1 (Ref 21).

Table 1 Nominal chemical composition of the cast iron samples (wt.%)

Element	G3500 (gray)	D4512 (ductile)
C	2.8-3.5	3.25-3.75
Si	1.5-2.2	2.25-2.60
Mn	0.7-1.0	0.2-0.5
Cr	0.35-0.50	0.25 max
Mo	0.35-0.50	…
Ni	…	0.5-1.0
Cu	0.7 max	…
S (max)	0.15	0.15
P (max)	0.15	0.08

The samples were polished with Emery paper. A 400-grit paper was used in the final stage, as recommended by GM Corporation for finishing dies used in metal stamping applications (Ref 22). The surface roughness parameters for the samples were measured with a profilometer and are shown in Table 2. The data were produced from the same area of each sample that was later used for surface roughness evaluation after nitrocarburizing processing.

The ductile iron sample had a slightly rougher surface after preparation with 400-grit paper, probably because of its softer ferrite matrix grains, compressed under the polishing pressure, have sprung back afterwards more, as compared to the pearlitic matrix of the gray cast iron sample, which responded to polishing differently since modulus of elasticity of graphite is about 7 GPa on average compared to 205 GPa of iron (Ref 23).

2.2 Processing Details

Gas nitrocarburizing experiments were carried out in a furnace made by Surface Combustion, equipped with software and electronics from Stange Elektronik GmbH for automatic control of the nitriding and carburizing potentials of the atmosphere. Plasma nitrocarburizing experiments were conducted in a system developed by Advanced Heat Treat Corp. with a cathodic heating shield and a pulse plasma generator of 6 kHz frequency.

Parameters in both processes were intentionally selected to enhance extreme conditions of the experiments. This was done to increase penetration of surface cavities, cracks, etc., by the compound zone (white layer) rather than to provide an optimized cycle for solving practical problems.

Also, the processing parameters of the gas nitrocarburizing process deviated from the optimum values recommended by the AMS 2759/12A (Ref 24). This specification does not distinguish between gray and cast irons in providing the optimum results. In selecting the processing detail, special care was taken to produce approximately the same thickness of about 10-14 μm of the compact portion of the compound zone in both gas and plasma processes. Heating (ramping) in the gas process to the final temperature was carried out in pure ammonia at an initial nitriding potential of about $K_N = 560$ atm$^{-1/2}$ at 460 °C and ending potential of $K_N = 3.5$ atm$^{-1/2}$ at final temperature. Heating in the plasma process from room to the final temperature was performed in a mixture of 30% nitrogen and 70% hydrogen. Detailed information of the processing parameters is presented in Table 3.

Table 2 Roughness measurement results representing the initial surface condition of the gray and ductile iron samples

Parameter	G3500 (gray)	D4512 (ductile)
R_z, μm	1.47	2.21
	1.25	2.64
	1.40	3.07
	1.24	2.47
	1.37	1.60
Average	1.35	2.40
R_a, μm	0.10	0.20
	0.88	0.14
	0.12	0.28
	0.10	0.25
	0.10	0.15
Average	0.26	0.20
Peak count, peaks/in.	38	38
	18	25
	81	64
	43	25
	30	38
Average	42	38

3. Results and Discussion

Both plasma and gas nitrocarburizing processes increased the surface roughness of all cast iron samples. A significantly bigger effect on surface roughness, specifically for the gray iron sample, could be seen from the gas nitrocarburizing process compared to the plasma nitrocarburizing process. The ductile iron sample following the gas process was only slightly rougher than after the plasma process, as can be seen in Table 4.

To explain this, consideration should be given to the different thermal expansion rates of graphite and iron under the process' temperature and the roughness difference measured at 23 °C. The thermal expansivity difference between these microstructural components can explain the presence of voids at the graphite-matrix interface, along with the eruptive bulges generating the roughness profile.

The number of surface peaks per inch increased significantly more after plasma processing than after gas processing. Although plasma process produced more surface peaks, they were not as tall as the ones produced by the gas process. This can also be seen in profilograms of the surface in Fig. 3. It should be noted that some of the peaks are comparatively taller in both gray and ductile iron samples only after processing in the gas method.

Table 4 Surface roughness parameters of the gray and ductile cast irons after gas and plasma nitrocarburizing at 570 °C (1058 °F) for 4 h

	Process			
	G3500 (gray)		D4512 (ductile)	
Parameter	Gas	Plasma	Gas	Plasma
R_z, μm	21.92	4.82	10.85	5.78
	12.99	5.72	6.88	7.40
	11.74	5.05	7.17	5.57
	15.35	5.62	7.40	6.91
	12.51	5.90	8.56	4.22
Average	14.90	5.42	8.17	5.98
R_a, μm	4.16	0.66	1.26	0.69
	2.09	0.74	0.88	0.81
	1.89	0.66	0.91	0.63
	2.65	0.71	0.95	0.80
	1.96	0.57	1.03	0.56
Average	2.55	0.67	1.06	0.70
Peak count, peaks/in.	178	292	152	170
	254	488	145	246
	292	381	165	284
	272	323	152	330
	297	292	132	145
Average	259	355	149	235

Table 3 Details of the gas and plasma nitrocarburizing experiments for the ductile and gray cast iron samples

Process	Temperature, °C	Time, h	Nitriding potential K_N, atm$^{-1/2}$	Carburizing potential K_C, W	Total pressure, mbar	Partial pressure of nitrogen, mbar	Partial pressure of methane, mbar
Gas	570	4	3.5	0.24	1030	…	…
Plasma	570	4	…	…	2.90	1.45	0.058

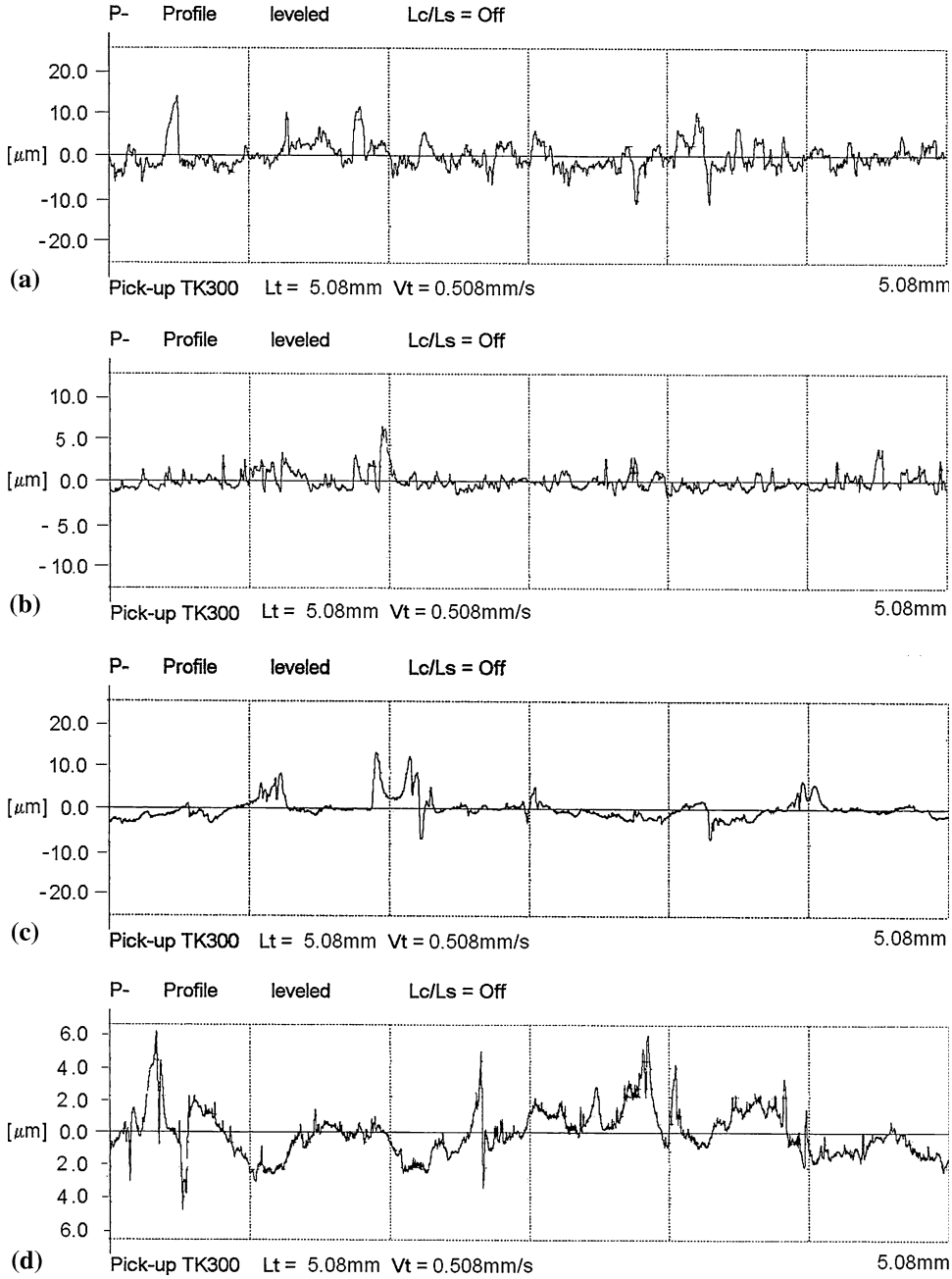

Fig. 3 Surface profilograms of the samples nitrocarburized at 570 °C (1058 °F). (a) Gray iron sample after gas processing, (b) gray iron sample after plasma processing, (c) ductile iron sample after gas processing, and (d) ductile iron sample after plasma processing

Scanning electron microscopy (SEM) pictures taken from surfaces of the samples show that the metallic components of the cast irons, either ferrite in ductile iron or pearlite in gray iron, are elevated above the surface in the areas where the graphite particles are located. This effect is much stronger in the gas compared to the plasma nitrocarburized samples as seen in Fig. 4. We verified that in the initial conditions of the samples, the graphite particles at the surface were also located slightly below the metallic matrix. In the case of ductile cast iron, some of the graphite nodules were also covered by fish-scale-like metallic particles (ferrite), which smeared over the surface during one-directional mode of the sample preparation.

Optical photomicrographs taken from cross sections of the samples show that the penetration of the compound zone (white layer) in the gray iron sample is much deeper locally, near graphite flakes, in the gas treated samples than it is in the plasma treated samples, resulting in the local elevation of the metallic components of the structure and rougher surface (Fig. 5a-d). A similar situation exists, but to a lesser degree is observed in the ductile iron sample processed in gas. Some of the graphite nodules were partially surrounded by the penetrating compound zone and were pushed outward, resulting in local bulges or cracks on the surface (Fig. 5c). Contrary to that, plasma processing of the ductile cast iron samples leaves open graphite particles on the surface and only small cracks of the matrix around them (Fig. 4g and h). The graphite nodules are either at the surface or hidden under the compound zone but generally they do not protrude above the surface. It is evident

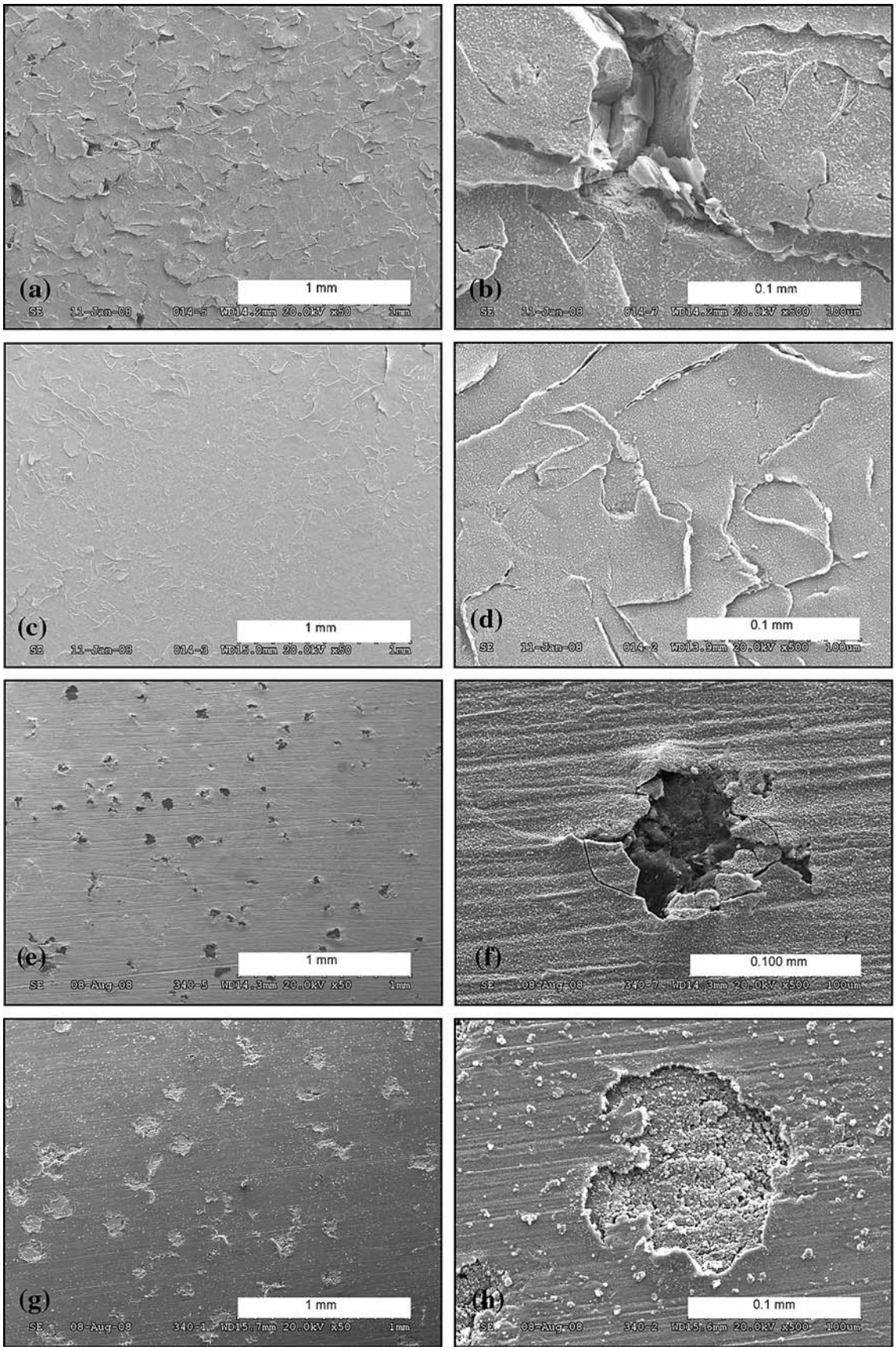

Fig. 4 SEM surface image of the samples nitrocarburized at 570 °C (1058 °F). (a, b) Gray iron sample after gas processing, (c, d) gray iron sample after plasma processing, (e, f) ductile iron sample after gas processing, (g, h) ductile iron sample after plasma processing

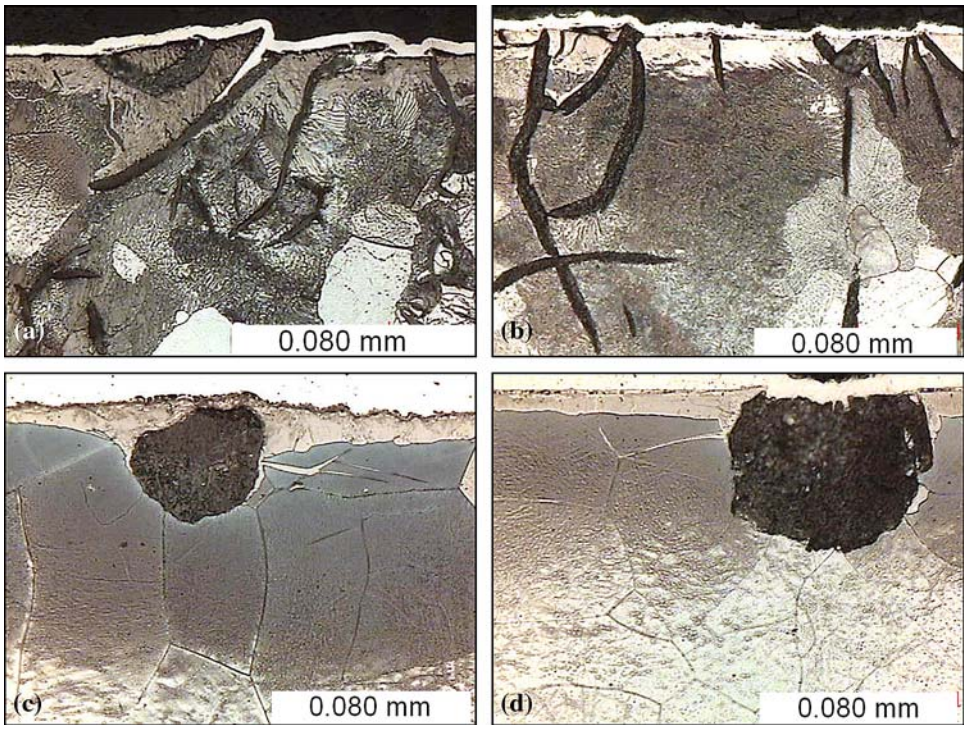

Fig. 5 Optical photomicrographs of the samples nitrocarburized at 570 °C (1058 °F). (a) Gray iron sample after gas processing, (b) gray iron sample after plasma processing, (c) ductile iron sample after gas processing, (d) ductile iron sample after plasma processing. Note the white layer on the surface is a nickel coating applied for a better edge retention of the samples during metallographic preparation. Etched with 3% nital

Table 5 Physical properties of the main structural components of the gray and ductile samples in nitrocarburized condition

Structural component	Density, g/cm^3	Specific volume, cm^3/g × 0.001	Coefficient of thermal expansion, 10^{-6}/K × 10^{-6}
Iron	7.88 (Ref 23)	127	11.7 (Ref 23)
Graphite	1.9 (Ref 23)	526	5 (Ref 23)
ε-$Fe_3(N_{0.32}C_{0.2})_{1.396}$ (Ref 27)	7.122	140	NA
ε-Fe_2N (Ref 27)	7.139	140	NA
ε-Fe_3N (Ref 25)	7.124	140	12 (for $Fe_3N_{1.00}$) 18 (for $Fe_3N_{1.22}$) (Ref 25)
γ′-Fe_4N (Ref 27)	7.241	138	NA

Density and specific volume of the nitrides was derived from the individual cells

through these results that the mechanism of plasma nitrocarburizing is not only different from the mechanism of gas nitrocarburizing process, but also the highly significant practical effects of this difference. Elevation of the structural components of the gray iron matrix above the surface appears to be caused by a locally much thicker compound zone resulting in deformation of the near-surface areas, probably caused by locally larger residual compressive stress arising during processing at elevated temperatures and thermally induced misfit between the layer and the substrate (Ref 25).

This is obviously a result of the larger specific volume of the nitrides forming the compound zone than the metallic matrix as well as the differences in the linear expansion of the structural components (see Table 5 for physical property details). Although no x-ray phase analysis was performed, it is very likely that the compound zone formed at 570 °C contained essentially two phases: ε + γ′ (Ref 26). At least portion of ε was enriched in carbon and formed ε-$Fe_3N(N,C)_{1+x}$. However, no specific data for linear expansion other compounds than that for ε-Fe_3N nitride could be found in the literature. It should be noted that thermal expansion of ε-Fe_3N could be smaller or larger than that of iron, depending on nitrogen content in its lattice (Ref 25). At higher nitrogen content, ε-Fe_3N expands more than the iron matrix and very likely the behavior of $Fe_3N(N,C)_{1+x}$ is similar.

It is clear that the situation caused by the differences in thermal expansion and different specific volumes of the phases present in the surface is very complex and more work is needed to separate the effect of various phenomena on the residual stress values and resulting surface deformation.

Table 6 Ratio of the after-process surface parameters of the gray and ductile cast iron samples to their initial values

Material	G3500 (gray)		D4512 (ductile)	
Process	Gas	Plasma	Gas	Plasma
Parameter				
R_z	11.0	4.0	3.4	2.5
R_a	9.8	2.6	5.3	3.5
Peak count	6.2	8.4	3.9	6.2

The fact is that the plasma process done at the same temperature produces a better product overall. The uneven thickness of the compound zone in the gas treated sample is a direct result of nitrocarburizing, occurring not only on the surface but also in the cavities and cracks penetrated by ammonia. In plasma processing, these tiny spaces between graphite flakes and the matrix were not penetrated by the active nitriding species, mainly N_2^+ ions, formed in plasma and therefore the thickness of the compound zone was more even.

There was not as dramatic a difference in the measured roughness, R_a and R_z parameters, of the surface between the ductile iron samples, either gas or plasma nitrocarburized. This seems to be an effect of less microstructural imperfection on the surface of the ductile iron and the limited ability of ammonia to penetrate these locations of the sample surface. The larger number of surface peaks in plasma treated samples suggests that the nucleation of the compound zone in the plasma method appears to be faster and more uniform than in the gas method. The heights of the surface peaks may perhaps also be limited in plasma method by sputtering affecting their growth. Redeposition of the sputtered atoms on the surface very likely helps to cover the surface voids, reducing the roughness.

4. Conclusions

The two different cast iron samples nitrocarburized in gas and plasma at 570 °C for 4 h responded differently to the treatments performed. The average compound zone thicknesses were almost identical; however, surface morphology and roughness values were different. Gas nitrocarburizing of the gray cast iron resulted in significantly increased surface roughness compared to the plasma treated samples. For the results, see Table 6.

For practical applications, the gasnitrocarburizing process has to be very carefully optimized to produce the layers of limited surface roughness, specifically in gray cast irons. In comparison, the plasma process, even if performed at such intentionally extreme condition as in our experiments (mainly in high temperatures), produces comparatively smooth surfaces, requiring less if any preparation of the product before its application.

Acknowledgments

The authors thank Dr. Witold Liliental at Nitrex Metal Technologies Inc., Burlington, Ontario, for his help with the metallography and Henry Zmijewski at the U.S. Steel Automotive Center, Troy, Michigan, for his help with SEM. The help of Dr. George Tymowski of Ottawa and Andrew Paczuski of Ann Arbor for their comments and suggestions is also greatly appreciated.

References

1. E. Roliński, A. Konieczny, and G. Sharp, Influence of Nitriding Mechanisms on Surface Roughness of Plasma and Gas Nitrided/Nitrocarburized Gray Cast Iron, *Heat Treat. Prog.*, 2007, March/April, p 39–46
2. D. Wells, Ion Nitriding: Only the Best 'Case' for Gas Compressors, *Heat Treat. Prog.*, 2001, August/September, p 45–46
3. A.U. Seybolt, Some Observations on the Metallurgy of Ion Nitriding, *Trans. Metall. Soc. AIME*, 1969, **245**, p 769–778
4. G.G. Tibbets, Role of Nitrogen Atoms in "Ion-Nitriding", *J. Appl. Phys.*, 1974, **11**(45), p 5072–5073
5. K. Keller, Schichtaufbau glimmnitrier Eisenwerkstoffe (Layer Structure of Ion-Nitrided Iron Alloys), *Härterei Technische Mitteilungen*, 1971, **26**, p 120 (in German)
6. M. Hudis, Study of Ion-Nitriding, *J. Appl. Phys.*, 1973, **4**(44), p 1489–1496
7. B. Edenhofer, Physical and Metallurgical Aspects of Ionitriding, *Heat Treat. Met.*, 1974, **2**, p 59–67
8. T. Karpiński and E. Roliński, Mechanismus des lonennitrieren (Mechanism of Ion Nitriding), *Celostatne Dni Tepelneho Spracovania*, Bratislava, 1978, *Czechoslovak Scientific and Technical Society, CVSVTS*, p 27–35 (in German)
9. H. Michel, T. Czerwiec, M. Gantois, D. Ablitzer, and A. Ricard, Progress in the Analysis of the Mechanisms of Ion Nitriding, *Surf. Coat. Technol.*, 1995, **72**, p 103
10. C.X. Li, T. Bell, and H. Dong, Study of Active Screen Plasma Nitriding, *Surf. Eng.*, 2002, **18**(3), p 174–181
11. J. Walkowicz, On the Mechanisms of Diode Plasma Nitriding in N_2-H_2 Gas Mixtures Under DC-Pulsed Substrate Biasing, *Surf. Coat. Technol.*, 2003, **174–175**, p 1211–1219
12. E. Roliński and G. Sharp, When and Why Ion Nitriding/Nitrocarburizing Makes Good Sense, *Ind. Heat.*, 2005, August, p 67
13. H.-J. Spies, H. Le Thien, and H. Biermann, Verhalten von Stählen beim Plasmanitrieren mit einem Aktivgitter (Behavior of Steels in Active Screen Plasma Nitriding), *HTM, Z. Werkst. Wämebeh. Fertigung*, 2005, **60**(4), p 1–8 (in German)
14. S.C. Brown, *Basic Data of Plasma Physics*, American Vacuum Society Classics, Ed. American Institute of Physics, New York, 1993, p 275
15. H.J. Grabke, Reaktionen von Ammoniak, Stickstoff und Wasserstoff an der Oberflache von Eisen, 1. Zur Kinetik der Nitrierung von Eisen mit NH_3-H_2-Gemischen und der Denitrierung (Reactions of Ammonia, Nitrogen and Hydrogen at the Surface of Iron in Ammonia-Hydrogen Mixes and Denitriding), *Berichte der Bunsengesellschaft*, 1968, **72**(4), p 533–541 (in German)
16. E. Roliński, Ion Nitriding and Nitrocarburizing of Sintered PM Parts, *Ind. Heat.*, 2004, October, p 33–35
17. E. Roliński, G. Sharp, K. Brondum, and N. Peterson, P/M Turbo Charger and Armature Components: Plasma Nitriding and Nitrocarburizing to Reduce Friction Wear, 2005 SAE World Congress, Detroit, MI, *Proc.*, April 11–14, 2005 (Warrendale, PA), SAE International, p 2005-01-0722
18. *Metals Handbook*, Properties and Selections: Irons, Steels and High Performance Alloys, Vol 1, 10th ed. ASM International, 1990
19. *Metals Handbook*, Machining, Vol 16, 9th ed. ASM International, 1989
20. T. Morishita, T. Hattori, Y. Kawado, and K. Tarumoto, Nitrided Cast Iron Products and Method for Manufacturing the Same, United States Patent, 4482399, 1984
21. *Global Standard Components*, NAAMS, Index for Stamping Dies Cast Materials, Auto/Steel Partnership, 10/29/07. www.naamstandards.org
22. D.J. Meuleman, Private communication on: GM Body Manufacturing Engineering, *Interim Specification for Ion (Plasma) Nitride Surface Treatment for Stamping Dies*, 2006
23. Van Vlack, *Elements of Materials Science & Engineering*, 4th ed. Addison-Wesley Publishing Company, 1980, p 523
24. ASM 2759/12, *Gaseous Nitrocarburizing, Automatically Controlled by Potentials*, Issued July 2007. http://www.sae.org

25. T. Gressman, A. Leineweber, and E.J. Mittemeijer, X-Ray Diffraction Line-Profile Analysis of Hexagonal ε-Iron Nitride Compound Layers: Composition- and Stress-Depth Profiles, *Philos. Mag.*, 2008, **88**(2), p 145–169
26. M. Nikolussi, A. Leineweber, E. Bischoff, and E.J. Mittemeijer, Examination of Phase Transformations in the System Fe-N-C by means of Nitrocarburizing Reactions and Secondary Annealing Experiments; the α + ε Two-Phase Equilibrium, *Int. J. Mater. Res.*, 2007, **98**(11), p 1086–1092
27. X-Ray Diffraction Data, International Centre for Diffraction Data, 2008, 12 Campus Boulevard, Newtown Square, PA 1907-3273. http://www.icdd.com